Polarization splitting phenomenon of photonic crystals constructed by two-fold rotationally symmetric unit-cells

Polarization splitting phenomenon of photonic crystals constructed by two-fold rotationally symmetric unit-cells

U G Yasa[1], I H Giden[1], M Turduev[2] and H Kurt[1]
[1] Nanophotonics Research Group, Department of Electrical and Electronics Engineering, TOBB University of Economics and Technology, 06560 Ankara, Turkey
[2] Photonic Networks Research Group, Department of Electrical and Electronics Engineering, TED University, 06420 Ankara, Turkey

E-mail: gorkemyasa@etu.edu.tr

Abstract. We present an intrinsic polarization splitting characteristic of low-symmetric photonic crystals (PCs) formed by unit-cells with C_2 rotational symmetry. This behavior emerges from the polarization sensitive self-collimation effect for both transverse-magnetic (TM) and transverse-electric (TE) modes depending on the rotational orientations of the unit-cell elements. Numerical analyses are performed in both frequency and time domains for different types of square lattice 2-fold rotational symmetric PC structures. At incident wavelength of λ=1550 nm, high polarization extinction ratios with ~26 dB (for TE polarization) and ~22 dB (for TM polarization) are obtained with an operating bandwidth of 59 nm. Moreover, fabrication feasibilities of the designed structure are analyzed to evaluate their robustness in terms of the unit-cell orientation: For the selected PC unit-cell composition, corresponding extinction ratios for both polarizations still remain to be over 18 dB for the unit-cell rotation interval of θ=[40°-55°]. Taking all these advantages, 2-fold rotationally symmetric PCs could be considered as an essential component in photonic integrated circuits for polarization control of light.

Keywords: Photonic crystals, polarization beam splitter, rotational symmetry, low-symmetry

1. Introduction

A variety of the photonic devices is designed to operate under a single polarization and thus, separating unpolarized wave into polarization states becomes essential. For this reason, polarization beam splitters (PBSs) could be considered as one of the essential components in the area of optics and photonics in order to split electromagnetic waves into two orthogonal polarization states, namely, transverse-electric (TE) and transverse-magnetic (TM) modes. Such devices are utilized in various applications such as optical communications, optical logic circuits and optical biosensors. Previously proposed PBS devices [1-5] do not meet the requirements of the today's optical circuits since their dimensions are on the order of millimeters. However, introduction of PCs into the literature has enabled more practical PBS designs comparing to conventional ones in terms of feasibility and compactness. Photonic crystal (PC) based PBS concepts and designs have already been studied in Refs. [6-14]. For instance, Solli *et al*. have played an important role in using the PBG feature of the PCs to filter out one of the two polarizations and transmit the other [6]. In addition, Zabelin *et al*. combined the PBG property with the

polarization insensitive self-collimation phenomenon and separated TM and TE polarizations in different propagation directions with the help of splitting PBG region placed in a PC heterostructure [7]. Since such type of heterostructure is composed of different PC media, corresponding PBS performance may be degraded adversely depending on possible fabrication errors. Another pioneering PBS concept was proposed by Wu *et al.* using different dispersion characteristics of both TM and TE modes [9]. In this PBS concept, however, since propagating polarized waves are exposed to light diffraction, there is no strong light confinement in the structure, and hence, an immense decrease in the transmission efficiency exists for both polarizations. Apart from the above-mentioned approaches, Ao *et al.* proposed polarization splitting effect using positive refractive index for one type of polarization and negative refractive index for the other [11]. However, precise oblique light incidence is required in such devices to excite the polarization sensitive index of PC. This necessity makes this PBS concept hard to embed into photonic integrated circuits. Furthermore, severe light scattering emerges at the air-PC interface due to the tilted source excitation, which leads to reduction in the transmission efficiency for both polarizations. In addition, apart from the PC based applications, other concepts that use different characteristics of light-matter interaction are also investigated in the current literature. For instance, recently studied PBS devices are generally based on the directional couplers (DCs) that use polarization sensitive coupling lengths of the incident light [15-21]. However, DC-based devices require a high-resolution fabrication processes due to the necessity of arranging two adjacent waveguides precisely.

In this study, different from previously reported device concepts we analyze a polarization splitting technique for different PC unit-cell compositions by utilizing polarization sensitive dispersive behavior of 2-fold symmetric PCs. As already known, photonic lattices are formed by the repeated arrangements of a simplest component, which is called as PC "unit-cell". Structural parameters of the PC unit-cells are the main determinant that influences the optical response of a periodic array to the incident light waves. Especially, rotational symmetry is one of the structural properties that specifies the spatial configuration of a PC unit-cell structure. In general, the order of rotational symmetry of an object is determined by how many degrees it has to be rotated to make it appear the same [22, 23]. Therefore, different unit-cell structures can be grouped (e.g. C_1, C_2, C_3) according to the rating of rotational symmetry they possess. For instance, C_2 type, i.e. 2-fold symmetric, unit-cell compositions have the same appearance after a rotation of 180° and the number "2" here means the ratio of the full rotation (360°) to 180°. A majority of the PC-based applications in the literature consist of PC unit-cells with circular rods or holes, which are highly symmetric in terms of rotational symmetry. On the other hand, structural modifications (e.g. replacement of circular rods with elliptical ones or insertion of an additional rod in a unit-cell geometry) on these PC unit-cells generate low-symmetric unit elements [24]. Thanks to their anomalous dispersion properties, low-symmetric PCs reveal inherent extraordinary optical characteristics, such as tilted or broad-angle self-collimation [25, 26], beam focusing [27], diffraction-free light propagation [28], wavelength-demultiplexing [29], coupled mode selection [30], band-gap enlarging [31], anisotropic zero-index mediums [32], and polarization sensitive devices [33]. The recent study in Ref. [33] presents an insight of PBS device design exploiting homogenous rectangular PCs. In this work, however, the polarization splitting effect is generalized to whole C_2 type PC unit-cells and comparative analyses among PCs with different geometries are also conducted.

The rest of the paper is organized as follows: spectral as well as time domain analyses of PCs` polarization splitting property are performed in Section 2. In Section 3, comparative analyses of different PC

unit-cell geometries are conducted in terms of polarization splitting performance. Finally, the outcomes of the study are summarized in the conclusion section, Section 4.

2. Time and spectral domain analyses of polarization splitting behavior

In order to show the polarization splitting ability of 2-fold rotationally symmetric PCs, firstly we have selected the square array of the unit-cells with elliptically shaped air-holes. The elliptical shapes are one of the simplest geometries among the C_2 symmetry group. Therefore, initially, unit-cells composed of elliptically shaped air-holes are analyzed for the polarization splitting characteristic of 2-fold rotational symmetric PCs. Figure 1(a) shows the $a \times a$ sized unit-cell composition of this PC structure and permittivities of the dielectric background and air-hole are selected as ε_b=12 (Si) and ε_a=1 (Air), respectively.

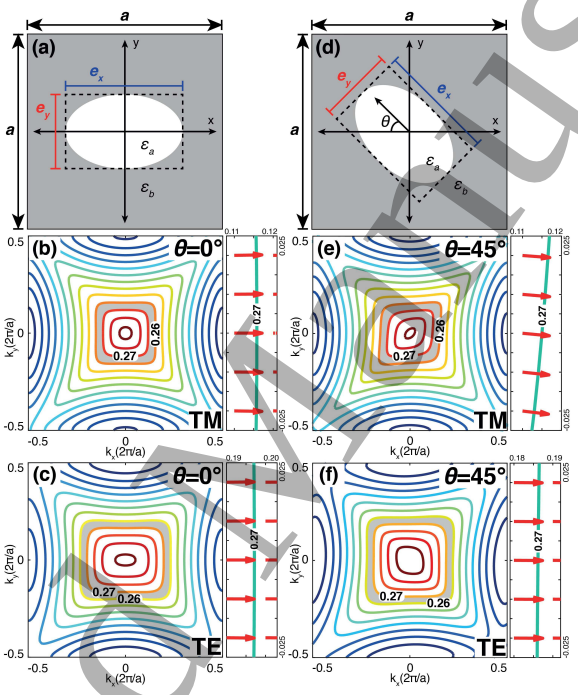

Figure 1. (a) Geometric representation of the low-symmetric unit-cell that consists of an elliptically shaped hole with dimension parameters e_x and e_y equal to 0.600a and 0.382a, respectively. (b) TM and (c) TE polarization iso-frequency contours (IFCs) corresponding to the given unit-cell configuration in (a). (d) The geometric representation of the same unit-cell when the air-hole orientation angle equal to θ=45° and related IFC figures for (e) TM and (f) TE polarizations. For the given unit-cells, permittivity constants are ε_a=1 and ε_b=12. Operating frequency bandwidth of the PBS device is shaded with gray color in all IFC figures.

Structural dimensions of the elliptical hole are e_x=0.600a and e_y=0.382a where lattice constant is a=411 nm and air filling ratio is F_a=18%. Throughout the study, plane wave expansion method is utilized to investigate the dispersion characteristics of the low-symmetric PC unit-cells [34]. The analysis of iso-frequency contours (IFCs) of the PC unit-cells gives information about light propagation within the photonic structure. Figures 1(b) and (c) represent the IFCs of the 2nd TM and TE polarization bands of the investigated PC unit-cells shown in figure 1(a). As can be seen from the figures 1(b) and (c), there exist flat dispersion contours for both TM and TE polarizations in the frequency interval of a/λ =[0.260-0.270] (gray-shaded area). This phenomenon asserts the polarization insensitive conventional self-collimation effect in ΓX propagation direction inside the PC medium. The direction of such a self-guiding light can be tuned by adjusting angular orientations of the PC unit-cells. For this reason, the given elliptical air-holes are rotated by an angle of θ=45° as shown in figure 1(d). Here, the θ parameter corresponds to the angular orientation of the air-holes and the reason to select θ=45° is explained later

in the following sections. Figures 1(e) and (f) represent the calculated IFCs for both TM and TE polarizations that correspond to the PC unit-cells given in figure 1(d). As can be seen from the figure 1, the changes in the axial rotations of the elliptical unit-cell elements give rise to an obliqueness in TM self-collimation contours (see figure 1(e)) while the TE ones are not affected much (see figure 1(f)). The emerging inclination in TM polarization IFCs reveals tilted self-collimated beam propagation since the gradients of IFCs indicate the light propagation direction at related normalized frequencies (see the gradient vectors in figure 1). On the other hand, TE polarized IFCs maintain their square-like shapes despite the change of air-hole rotation angle and conventional self-collimation feature still exists in the same normalized frequency interval. Such polarization-sensitive self-collimation property can be used for polarization splitting purpose without introducing any additional structural defects inside the PC medium. The given lengths of the minor and major axes of elliptical PC holes in figure 1 are selected by applying a structural parameter sweep and extracting the IFC distributions of TM and TE polarizations for each configuration when the PC air-hole orientation equals to θ=45°. During the parameter sweeping process, the unit-cells corresponding to the scanned structure parameters are selected to include an overlapped self-collimation frequency interval for both polarizations in their band structures. Then it is determined that the unit-cell structure having the highest contour inclination (consequently better polarization splitting performance) in the IFC distribution of TM polarization belongs to the unit-cell case with parameters e_x=0.600a and e_y=0.382a. In addition, polarization splitting phenomenon of 2-fold rotational symmetric unit-cells is obtained by utilizing configurations with air-holes in a high-index background. However, for the complementary case of high-index rods in an air background, no overlapped frequency intervals between TE and TM polarizations exist, which prevents us to use dielectric rods instead of air-holes in the proposed PBS concept.

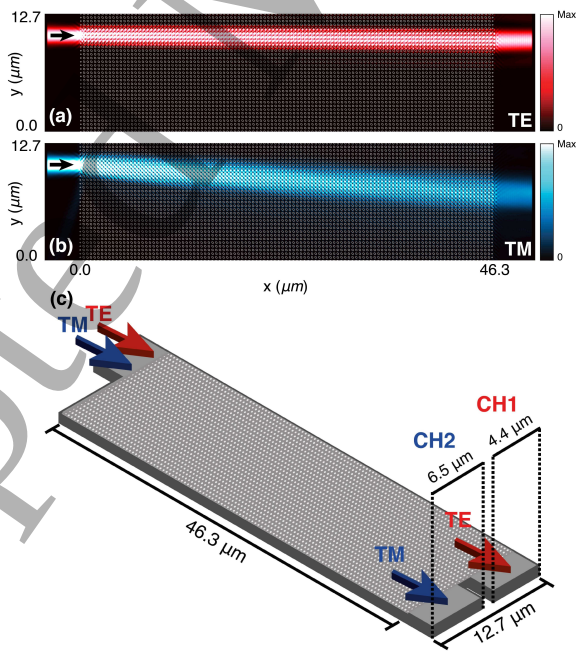

Figure 2. Spatial intensity distributions of the low-symmetric PC medium (consists of elliptical holes) for (a) TE and (b) TM polarizations at normalized frequency a/λ=0.265. (c) 3D representation of the proposed PBS device together with its output channels CH1 (TE) and CH2 (TM). Channel dimensions are arranged to obtain maximum performance (transmission & extinction ratio) from the different unit-cell configurations which will be discussed in the later parts of this paper.

Finite-difference time-domain (FDTD) method is used to numerically investigate time-domain response of the designed PC structure [35]. Figures 2(a) and (b) are prepared to demonstrate spatial intensity distributions inside the low-symmetric PC medium for both TE and TM polarization states at a/λ=0.265, respectively. Corresponding PC structure is composed of 45° rotated elliptical PC air-holes. In compliance with the IFC calculations presented in figures 1(e) and (f), expected conventional self-collimation phenomenon can be observed for TE polarized light (see figure 2(a)) whereas the TM polarized light has a tilted light propagation inside the periodic medium, see figure 2(b). In both polarizations, thanks to the self-collimation effect, incident beam propagates in diffraction-free manner, which enhances the polarization separation performance at the output ports in terms of transmission and retaining the mode profile. Relying on the presented results, one can deduce that an efficient splitting of two orthogonal light polarizations can be achieved using rotated elliptical PC air-holes. In addition to the elliptical ones, the polarization splitting characteristic can be generalized to whole C_2 symmetric unit-cell configurations, as well. In order to transform the proposed extraordinary self-collimation phenomenon into PBS application, input and output ports are introduced to the given PC medium, see the 3D illustration of PBS device in figure 2(c). The designed PBS device has CH1 (TE) and CH2 (TM) output ports with widths of 4.4 μm and 6.5 μm, respectively. The channel dimensions are arranged to obtain optimum polarization splitting performance from different types of C_2 symmetric PC unit-cells. The structural dimensions of intended PBS device are fixed to be 46.3 μm × 12.7 μm with lattice constant equal to a=411 nm.

3. Discussion and evaluation of numerical results

In this section, additional three 2-fold symmetric unit-cell configurations having the same filling ratios, namely {U2, U3, U4}, are analyzed to demonstrate the freedom of unit-cell selection within C_2 symmetry group.

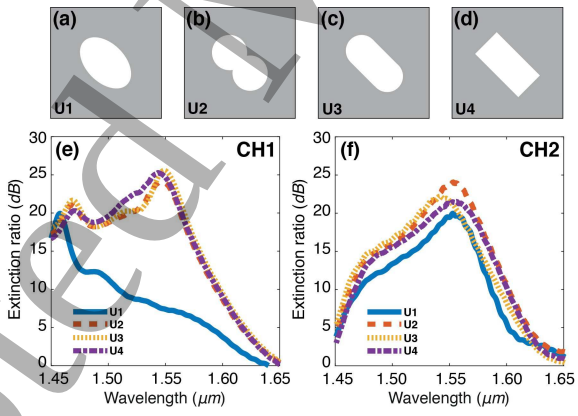

Figure 3. The unit-cell representations of different air-hole compositions with 2-fold rotational symmetry: (a) U1 (elliptical), (b) U2 (overlapped circles) (c) U3 (rounded rectangle) and (d) U4 (perfect rectangle). The dimensions of the each air-hole geometry are selected to have same air filling ratio (F_a=18%) in unit-cell scale. Polarization extinction ratio curves at CH1 (TE) and CH2 (TM) output ports of the PBS devices composed of the given unit-cell configurations in (a)-(d). Each unit-cell is represented with different color and line style.

The reason for selecting unit-cells with same air filling ratios (F_a ≈18%) is to compare their polarization separation performance by keeping their operating PBS frequency interval the same. Figures 3(b)-(d) represent the selected PC air-holes; U2 (overlapped circles), U3 (rounded rectangle) and U4 (perfect rectangle), respectively. It should also be noted that C_2 symmetric unit-cell designs are not limited to these ones and can be further expanded with different compositions, as well.

In order to analyze the polarization splitting performance of the four given PC unit-cell geometries in figures 3(a)-(d), corresponding polarization extinction ratios (PERs) are calculated at the output ports CH1 and CH2. The PER is defined as the ratio of the transmission efficiencies between the requested and unwanted polarizations at an output channel in dB scale. The PER values at each output channel are calculated by the following relation:

$$PER_{CH\#}=10\log_{10}(T_{requested}/T_{unwanted}) \quad (1)$$

where, $T_{requested}$ corresponds to the transmission of the desired polarization state whereas the $T_{unwanted}$ defines the transmission of unwanted polarization state at an output port. In this case, to calculate the PER_{CH1}, $T_{requested}$ is determined as the transmittance of the TE polarization and $T_{unwanted}$ describes the transmittance of the TM mode at CH1 port. Figure 3(e) shows the PER efficiencies at CH1 port within incident wavelengths 1.45 μm–1.65 μm. Similarly, figure 3(f) represents the extinction ratio curves for the four unit-cell compositions at CH2 port within the same wavelength interval. In both graphs, PER curves were represented with different colors and dash styles corresponding to specified unit-cell structures. As can be seen from the figure 3(e), extinction ratio curves at the CH1 ports of the PBS devices generated by C_2 group unit-cells (U2, U3 and U4) show almost identical fluctuations to each other except for the U1 type PC unit-cell. The main reason of the low PER_{CH1} performance of the unit-cell U1 lies in the IFC shapes of the elliptically shaped air-holes. The polarization separation at the end of the structure is comparably low because the inclination of the TM polarization IFCs of the elliptical holes is less than the other types of unit-cells {U2, U3, U4}. In this case, high cross-talk occur between the channels which is undesired and that causes corresponding PER_{CH1} value to decrease. On the other hand, for the other PC unit-cell configurations, PER_{CH1} is relatively high because of the higher inclination of the TM mode IFCs within the interested wavelengths. Examining the PER calculations in figure 3(f), large difference in the PER_{CH1} is not observed in PER_{CH2} case in comparison with elliptically shaped holes. Such stability in PER_{CH2} may be attributed to the fact that the slope reduction in the TM polarization IFCs has no effect on the TE transmission efficiency at the CH2 output port.

Table 1. Transmission and PER efficiencies at the proposed device's output at operating wavelength λ=1550 nm for the PCs consisting of the given unit-cell compositions when θ=45°.

Unit-cell	Transmission TE (CH1)	Transmission TM (CH2)	PER_{CH1} (dB)	PER_{CH2} (dB)
U1	92.8 %	30.3 %	7.4	19.6
U2	92.8 %	71.1 %	23.9	23.8
U3	87.7 %	72.5 %	25.5	21.5
U4	93.0 %	73.9 %	24.7	21.3

Table 1 shows the transmission and PER performance values at λ=1550 nm of the proposed device composed of the {U1, U2, U3, U4} PC unit-cells. As expected from the figures 3(e) and (f), the polarization splitting performance in the unit-cell U1 case is at the lowest level because of the reduced TM transmission at CH2 output port. On the other hand, the transmission efficiencies of PBS devices with the unit-cells U2, U3 and U4 are calculated at the CH1 (CH2) output port and have the values over 85% (71%). Corresponding efficiencies higher than the U1 case ensure that the PER_{CH1} and PER_{CH2} values are greater than 20 dB at both ports for the

cases of {U2, U3, U4} unit-cells so that an efficient polarization separation could be obtained at the output ports. U3-type unit-cell is selected among the investigated PCs due to its polarization splitting performance and the fabrication feasibility: Sharp cornered structures such as U2 and U4 are difficult to realize since a high-resolution nanofabrication process is required. On the other hand, fabricating the PC unit-cell of type U3 is more feasible due to its rounded corners. Since low-symmetric unit-cells behave differently in spectral domain with respect to their axial orientation angles, polarization separation performance of the selected U3-type unit-cell should be analyzed for each θ rotation parameter to find the optimum case. Figure 4(a) shows corresponding PER_{CH1} and PER_{CH2} efficiencies at operating wavelength λ=1550 nm (represented with the orange-square and blue-circular markers, respectively) while rotating the PC unit-cells between the angles of 0° and 90° with 5° steps. The schematics of PC unit-cells with certain θ values are also given as insets in the same figure. In addition, structural dimensions of the air-hole are given in the schematic inset that corresponds to the θ=0°. As can be deduced from the figure 4(a), corresponding PER values at both output ports give an almost sinusoidal response with respect to the rotation angle of the PC air-hole. As can be seen from the plot, the inclination of the frequency contours in TM polarization IFCs reaches its maximum value in the vicinity of θ=45°. Therefore, the rotation angles of the unit-cell holes are selected to be θ=45° to obtain maximum polarization splitting performance. Figures 4(b) and (c) show IFC distributions of the unit-cell U3 case for TM and TE polarization states when the air-hole orientation equals to θ=45°, respectively. Comparing to the elliptical hole case in figure 1(e), inclination amount in the TM polarization IFC lines of unit-cell U3 is greater, which shows the higher performance of the unit-cell U3 over U1 case in Table 1. Figure 1(a) indicates that the PER_{CH1} maintains its value above 20 dB level for the rotation interval of θ=[35°-55°] and the PER_{CH2} parameter stays beyond the 18 dB in the interval of θ=[40°-60°]. In accordance with these results, one can infer that the polarization separation performance is considerably high for a wide rotation range. In this way, the proposed PBS device may still operate at tolerable performance even possible angular orientation errors occur during the fabrication process.

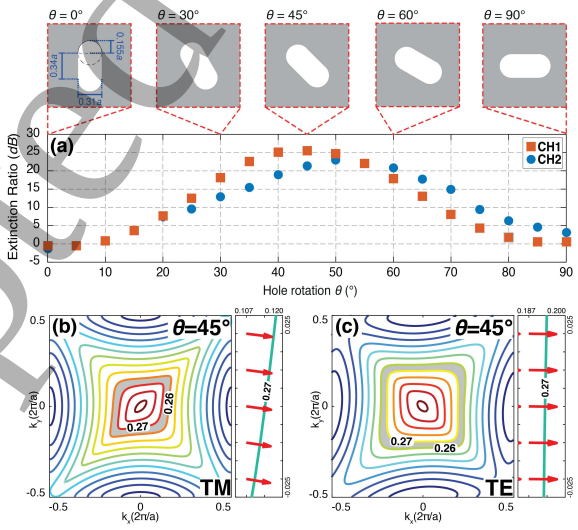

Figure 4. (a) The alteration of the polarization extinction ratios at λ=1550 nm which corresponds to the different angular orientations (θ=[0°-90°]) of the rounded-rectangular hole. The extinction ratio values for output channels CH1 and CH2 are represented with orange-square and blue-circular markers, respectively. Dimensions of the hole are presented in the inset which belongs to the θ=0° case. (b) TM and (c) TE polarization IFCs corresponding to the rounded-rectangular hole case when air-hole rotation equals to θ=45°.

The PER efficiencies of the proposed PBS device were given at a single wavelength (λ=1550 nm) so far. Nevertheless, the operational bandwidth is also an important factor for photonic applications. In the optical C-band range (1530 nm – 1565 nm), PER_{CH1} and PER_{CH2} values of U3 unit-cell case are more than 20.7 dB and 17.96 dB, respectively. In addition, examining figures 3(e) and (f), it is observed that other PC unit-cell compositions except for U1 have almost the same performance in the optical C-band range. The operational bandwidth that the device exhibits polarization separation ability is $\Delta\lambda$=59 nm, which corresponds to the normalized frequency interval a/λ=[0.260 – 0.270] for the given lattice constant.

The intensity distributions of the proposed photonic device consisting of the unit-cell U3 are calculated at the normalized frequency of λ=1550 nm and the results are shown in figures 5(a) and (b) for both TE and TM polarization states, respectively. Compared with the PBS device consisting of elliptical air-holes (see figures 2(a) and (b)), it is observed that the degree of polarization separation is higher for the unit-cell U3 case. As mentioned earlier, this is due to the fact that inclination in the TM polarization IFCs of the elliptical air-holes is less than the other unit-cell compositions. In order to analyze the exit points of the both TE and TM polarizations at the end of the structure, vertical cross sections of the output beams are superimposed in figures 5(c) and (d), respectively, for the wavelength interval of λ=[1467 nm – 1643 nm]. In both figures, vertical intensity distributions that correspond to the λ=1550 nm are represented with the white-dashed lines. When the incident frequency is increased, the tilting effect along –y axis in TM polarization is clearly seen in figure 5(d) whereas output beam shifts toward +y direction in TE polarization, see figure 5(c).

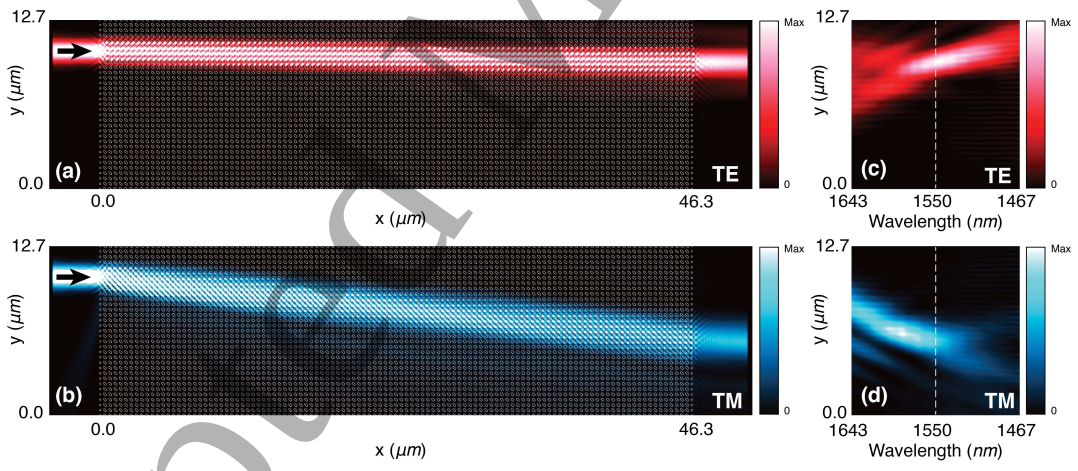

Figure 5. Spatial intensity distributions of the PBS device consisting of unit-cell U3 for (a) TE and (b) TM polarizations at λ=1550 nm. (c) TE and (d) TM power densities at the vertical cross-section of exit interface of the PBS device for the wavelength interval λ=[1467 nm – 1643 nm].

It is important to discuss the controllability of the separation angle of polarized waves in the proposed PBS configuration. The PBS approach proposed in this study is conceptually depends on extraordinary dispersion characteristics of PC structures having unit-cells with 2-fold rotational symmetry. As mentioned before, the main factor of the polarization splitting concept lies on the tilted and conventional self-collimation phenomena. Here, tilted self-collimation phenomenon, which guides light to propagate inclined inside the structure, is an inherent characteristic of C_2 symmetry group PCs. This property strongly depends on the angular orientations of the low-symmetric unit-cells and emerges from the tilted dispersion lines in their IFCs.

Obliqueness of the tilted self-collimated light propagating inside the structure can be controlled by tuning the rotations of the 2-fold symmetric PC unit-cells. In order to demonstrate the orientation dependent vertical alterations at the exit position of the propagating waves, output cross-sectional intensity distributions at λ=1550 nm are superimposed for PCs consisting of unit-cell U3, with respect to the unit-cell rotations for both TM and TE polarizations as shown in figures 6(a) and (b), respectively. As can be deduced from the intensity map in figure 6(a), when the angular orientation of the unit-cell is increased, an inclination starts to show up in dispersion contours of the TM polarization and exit position of the propagating light moves away from the initial position and gets its maximum shift in the vicinity of θ=45°. Here, amount of this inclination angle strongly depends on the value of the unit-cell rotation and gets its maximum value when the unit-cell is rotated by θ=45°, thus, maximum vertical shift at exit position appears. On the other hand, we know that the TE polarization dispersion contours are not affected much by the alterations in the unit-cell orientation. Therefore, exit positions of TE polarized waves are not affected much from the unit-cell rotation as shown in the figure 6(b). Thanks to this property, unit-cell orientation dependency of the TM polarized light can be exploited to control the TE/TM separation angle in proposed PBS concept. By doing this, different PBS devices can be designed to meet the structural requirements of photonic applications. Furthermore, emerging performance decreases in the PER values due to reduced separation angle can be compensated by adjusting the device length to obtain larger vertical distance between the output polarized beams.

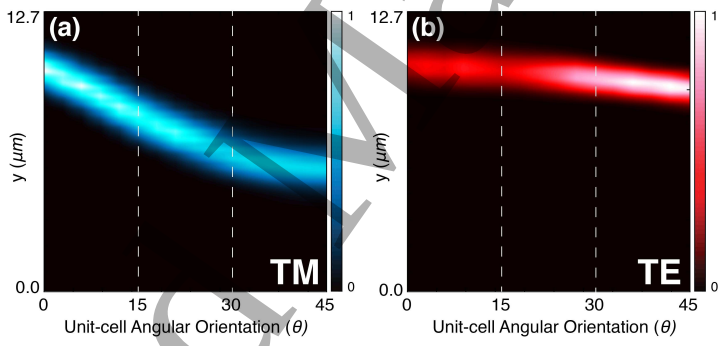

Figure 6. Vertical alterations in the output positions of the (a) TM and (b) TE polarization light intensities at λ=1550 nm at depending on the unit-cell orientations in the interval of θ=[0°-45°].

4. Conclusion

In the presented study, the rotationally dependent polarization splitting abilities of PC unit-cells having 2-fold rotational symmetry are examined. It can be inferred from the investigation of the dispersion characteristics for both TM and TE polarizations that polarization splitting in C_2 symmetric PC unit-cells is an inherent optical characteristic that provides the design of high extinction ratio PBS devices. In order to compare the polarization splitting efficiencies of low-symmetric PCs, FDTD analyses are implemented for the proposed PBS devices composed of C_2 type different PC unit-cells. Good polarization splitting performance is obtained by means of tilted self-collimation effect for three PC unit-cell types {U2, U3, U4} with PER efficiencies over 20 dB for both TM and TE polarizations, respectively, with operating bandwidth of 59 nm. Moreover, robustness of PBS design is analyzed depending the possible fabrication errors in unit-cell rotations. Corresponding PER calculations verify that high efficient PBS devices could be designed based on PCs with 2-fold symmetry in different geometries.

Acknowledgements

U.G.Y, I.H.G. and H.K. gratefully acknowledge the financial support from the Scientific and Technological Research Council of Turkey (TUBITAK), project 115R036. H.K. also acknowledges partial support of the Turkish Academy of Sciences.

References

[1] Albrecht P, Hamacher M, Heidrich H, Hoffmann D, Nolting H P and Weinert C M 1990 TE/TM Mode Splitters on InGaAsP/InP *IEEE Photonics Technol. Lett.* **2** 114–5

[2] Shani Y, Henry C H, Kistler R C, Kazarinov R F and Orlowsky K J 1990 Integrated optic adiabatic polarization splitter on silicon *Appl. Phys. Lett.* **56** 120–1

[3] Shiraishi K, Sato T and Kawakami S 1991 Experimental verification of a form-birefringent polarization splitter *Appl. Phys. Lett.* **58** 211–2

[4] Soldano L B, de Vreede A H, Smit M K, Verbeek B H, Metaal E G and Green F H 1994 Mach-Zehnder Interferometer Polarization Splitter in InGaAsP/InP *IEEE Photonics Technol. Lett.* **6** 402–5

[5] Oh M C, Lee M H and Lee H J 1999 Polymeric waveguide polarization splitter with a buried birefringent polymer *IEEE Photonics Technol. Lett.* **11** 1144–6

[6] Solli D R, McCormick C F, Chiao R Y and Hickmann J M 2003 Photonic crystal polarizers and polarizing beam splitters *J. Appl. Phys.* **93** 9429–31

[7] Zabelin V, Dunbar L A, Le Thomas N, Houdré R, Kotlyar M V, O'Faolain L and Krauss T F 2007 Self-collimating photonic crystal polarization beam splitter *Opt. Lett.* **32** 530–2

[8] Kim S, Nordin G P, Cai J and Jiang J 2003 Ultracompact high-efficiency polarizing beam splitter with a hybrid photonic crystal and conventional waveguide structure. *Opt. Lett.* **28** 2384–6

[9] Wu L, Mazilu M, Gallet J F, Krauss T F, Jugessur A and De La Rue R M 2004 Planar photonic crystal polarization splitter. *Opt. Lett.* **29** 1620–2

[10] Lu Z, Tang Y, Shen Y, Liu X and Zi J 2005 Polarization beam splitting in two-dimensional photonic crystals based on negative refraction *Phys. Lett. Sect. A Gen. At. Solid State Phys.* **346** 243–7

[11] Ao X and He S 2005 Polarization beam splitters based on a two-dimensional photonic crystal of negative refraction *Opt. Lett.* **30** 2152–4

[12] Liu T, Zakharian A R, Fallahi M, Moloney J V. and Mansuripur M 2005 Design of a compact photonic-crystal-based polarizing beam splitter *IEEE Photonics Technol. Lett.* **17** 1435–7

[13] Zhen Y R and Li L M 2005 A novel application of two-dimensional photonic crystals: polarization beam splitter *J. Phys. D. Appl. Phys.* **38** 3391–4

[14] Tserkezis C and Stefanou N 2011 Negative refraction in plasmonic crystals of metallic nanoshells Metamaterials 5 169–77

[15] Gao S, Wang Y, Wang K and E Skafidas 2016 Low-Loss and Broadband 2×2 Polarization Beam Splitter Based on Silicon Nitride Platform *Photonics Technol. Lett. IEEE* **28** 1936–9

[16] Hsu C W, Hang T K, Jhen-yu C and Cheng Y C 2016 8.13 μm in length and CMOS compatible polarization beam splitter based on an asymmetrical directional coupler *Appl. Opt.* **55** 3313–8

[17] Zhang T, Yin X, Chen L and Li X 2016 Ultra-compact polarization beam splitter utilizing a graphene-based asymmetrical directional coupler *Opt. Lett.* **41** 356

[18] Xu Y and Xiao J 2016 Design of a compact and integrated TM-rotated / TE-through polarization beam splitter for silicon-based slot waveguides *Appl. Opt.* **55**

[19] Zhang Y, He Y, Jiang X, Liu B, Qiu C, Su Y and Soref R A 2016 Ultra-compact and highly efficient silicon polarization splitter and rotator *APL Photonics* **1** 91304

[20] Wang J, Xiao J and Sun X 2013 Design of a compact polarization splitter composed of a multiple-slotted waveguide and a silicon nanowire *J. Opt.* **15** 35501

[21] Haldar R, Mishra V, Dutt A and Varshney S K 2016 On-chip broadband ultra-compact optical couplers and polarization splitters based on off-centered and non-symmetric slotted Si-wire waveguides *J. Opt.* **18** 105801

[22] Hamermesh M 1989 *Group theory and its application to physical problems* (New York: Dover)

[23] Glazer M and Burns G 2013 *Space groups for solid state scientists* (Amsterdam: Elsevier)

[24] Giden I H, Turduev M and Kurt H 2014 Reduced symmetry and analogy to chirality in periodic dielectric media *J. Eur. Opt. Soc.* **9**

[25] Turduev M, Giden I H and Kurt H 2012 Modified annular photonic crystals with enhanced dispersion relations: polarization insensitive self-collimation and nanophotonic wire waveguide designs *J. Opt. Soc. Am. B* **29** 1589

[26] Jiang L, Wu H and Li X 2013 Polarization-insensitive and broad-angle self-collimation in a two-dimensional photonic crystal with rectangular air holes *Appl. Opt.* **52** 6676–84

[27] Kurt H, Turduev M and Giden I H 2012 Crescent shaped dielectric periodic structure for light manipulation. *Opt. Express* **20** 7184–94

[28] Giden I H, Turduev M and Kurt H 2013 Broadband super-collimation with low-symmetric photonic crystal *Photonics Nanostructures - Fundam. Appl.* **11** 132–8

[29] Turduev M, Giden I H and Kurt H 2013 Extraordinary wavelength dependence of self-collimation effect in photonic crystal with low structural symmetry *Photonics Nanostructures - Fundam. Appl.* **11** 241–52

[30] Kilic O, Digonnet M, Kino G and Solgaard O 2008 Controlling uncoupled resonances in photonic crystals through breaking the mirror symmetry. *Opt. Express* **16** 13090–103

[31] Kuang W, Hou Z, Liu Y and Li H 2005 The bandgap of a photonic crystal with triangular dielectric rods in a honeycomb lattice *J. Opt. A Pure Appl. Opt.* **7** 525–8

[32] Wu Y 2014 A semi-Dirac point and an electromagnetic topological transition in a dielectric photonic crystal *Opt. Express* **22** 1906–17

[33] Yasa U G, Turduev M, Giden I H and Kurt H 2017 High extinction ratio polarization beam splitter design by low-symmetric photonic crystals *J. Lightw. Technol.* **35** 1677-83

[34] Johnson S and Joannopoulos J D 2001 Block-iterative frequency-domain methods for Maxwell's equations in a planewave basis *Opt. Express* **8** 173

[35] Oskooi A F, Roundy D, Ibanescu M, Bermel P, Joannopoulos J D and Johnson S G 2010 Meep: A flexible free-software package for electromagnetic simulations by the FDTD method *Comput. Phys. Commun.* **181** 687–702